

Bioinspired Nanostructured Lipid Carriers Functionalized with Keratin-Binding Peptides for Enhanced Transungual Delivery of Efinaconazole

Kshipra Rajput, Akhlesh K. Singhai

Department of Pharmaceutics, School of pharmacy, LNCT University, Bhopal, India.,,
kshipraruajput95@gmail.com

Abstract

In order to improve the transungual delivery of efinaconazole through nail keratin for the topical treatment of onychomycosis, this study sought to create bioinspired nanostructured lipid carriers (NLCs) functionalized with keratin-binding peptides. NLCs were formulated using the solvent evaporation technique with stearic acid and oleic acid, optimized via Box-Behnken Design (BBD), and surface-engineered using a decorin-derived peptide to mimic natural keratin-binding mechanisms. Characterization studies showed that it outperformed the plain drug ($90 \pm 2\%$ release in 24 hours) by having a particle size of 120 ± 6 nm, an entrapment efficiency (EE) of $88 \pm 2\%$, and a sustained drug release of $75 \pm 3\%$ over 72 hours. A depth of 1.2 ± 0.1 mm was found in *in vitro* nail penetration studies, which is almost twice as deep as unmodified NLCs (0.5 ± 0.1 mm, $p < 0.005$, one-way ANOVA). In antifungal tests against *Candida albicans*, the bioinspired NLCs' zone of inhibition (ZOI) was 28 ± 2 mm, while the plain NLCs' was 20 ± 1 mm ($p < 0.005$). Topical safety was supported by skin irritation studies that used the Draize test, which showed non-irritancy (score: 0.7 ± 0.2). These findings demonstrate how bioinspired NLCs may be used as a new, secure, and effective way to increase drug penetration through nail keratin and, consequently, improve treatment outcomes for fungal nail infections.

Keywords: Bioinspired NLCs, nail keratin, Efinaconazole, onychomycosis, drug penetration, topical delivery

1. INTRODUCTION

Candida albicans and dermatophytes like *Trichophyton rubrum* are the main culprits behind onychomycosis, a fungal infection of the nail plate and bed. About 10–20% of people worldwide are afflicted, with older adults and those with compromised immune systems having a higher prevalence [1]. According to clinical research, the thick, keratinized nail plate—which varies in thickness from 0.5 to 1 mm depending on anatomical location—causes recurrent infections in over half of afflicted patients [2, 3].

This keratin barrier, composed of tightly packed disulfide bonds and lipophilic domains containing 1–2% (w/w) lipids, presents a significant obstacle to effective topical drug penetration, often restricting absorption to a depth of only 0.1–0.5 mm [4,5]. Conventional topical treatments must therefore be applied frequently, which results in low patient compliance and treatment failure [6]. Despite their ability to reach deeper tissue concentrations, systemic antifungal medications such as itraconazole and efinaconazole have serious side effects, such as hepatotoxicity, gastrointestinal problems, and drug interactions, which makes them inappropriate for long-term use in patients with comorbidities [7, 8]. Due to their high drug-loading capacity, hybrid lipid matrix made of solid and liquid lipids, and nanoscale size (50–200 nm), nanostructured lipid carriers (NLCs) present a promising substitute [9-10]. In comparison to solid lipid nanoparticles (SLNs), their disordered inner structure allows for better drug entrapment, and their lipophilicity improves interaction with the lipid components of the nail, resulting in improved diffusion [11]. However, passive diffusion mechanisms that are unable to specifically target keratin-rich tissues limit the use of conventional unmodified NLCs, leading to low drug accumulation at the infection site [12] and suboptimal penetration depth. Bioinspired strategies, which imitate natural molecular recognition processes, have emerged as novel approaches to get around this restriction. Decorin, a tiny, leucine-rich proteoglycan present in

the extracellular matrix, is one such molecule that binds to keratin exclusively through conserved peptide domains.^{13, 14}. Motivated by this mechanism, the current study functionalizes NLC surfaces by increasing their affinity for nail keratin using a decorin-derived keratin-binding peptide. Efinaconazole can be delivered deeper and more precisely into the nail bed thanks to this modification, which is thought to strengthen peptide-keratin interactions through hydrogen bonding and hydrophobic forces [15, 16]. Therefore, the purpose of this study was to: (i) use a Box-Behnken Design to formulate and optimize bioinspired NLCs loaded with efinaconazole; (ii) describe their physicochemical properties and nail penetration efficiency; and (iii) assess their antifungal efficacy and dermal safety for possible topical treatment of onychomycosis. It is anticipated that this bioinspired drug delivery system will solve the clinical need for a safe, non-systemic, and patient-compliant therapy^{17, 18} and get past the difficulties presented by the nail's strong keratin barrier. NLCs' lipophilicity and deformability have demonstrated a great deal of promise for transungual drug delivery [30].

Receptor binding and tissue specificity are improved by peptide-based functionalization.³¹ Topical treatment for onychomycosis has demonstrated positive efficacy with finaconazole.³³ Keratin biomaterials are well-known for their regenerative qualities, structural resemblance to the natural extracellular matrix, and biocompatibility, which make them useful scaffolds for skin wound healing applications [39].

Despite the availability of many topical antifungal drugs, clinical outcomes vary depending on the patient's age and immunological status. Recent meta-analyses have shown that fluconazole and amphotericin B are better for adult patients, while miconazole is better for juvenile situations. These findings highlight the necessity of developing new antifungal delivery systems that more accurately target tissues and offer sustained release to boost efficacy and reduce recurrence [40].

2. MATERIALS AND METHODS

2.1 Materials

Efinaconazole ($\geq 98\%$ purity, confirmed by HPLC) provided the efinaconazole ($\geq 98\%$ purity, verified by HPLC). We purchased oleic acid (liquid lipid) and stearic acid (solid lipid; m.p. $\sim 69^\circ\text{C}$) from Sisco Chemicals Pvt. Ltd. in Mumbai, India. CDH Pvt. Ltd., India, provided Tween 80 (polyoxyethylene sorbitan monooleate; HLB = 15) and Carbopol 940 (cross-linked polyacrylic acid polymer). Mass spectrometry was used to characterize the decorin-derived keratin-binding peptide (sequence: LRELHLNNC; MW ~ 1 kDa; $\geq 95\%$ purity), which was custom synthesized by [GenScript, Piscataway, NJ, USA]..

Triethanolamine was utilized to adjust the pH, and analytical-grade acetone served as the organic solvent. To replicate nail bed conditions, phosphate-buffered saline (PBS, pH 6.8) was made internally. The Microbial Type Culture Collection (MTCC) in Chandigarh, India, provided the *Candida albicans* strain MTCC 227, which was cultivated on Sabouraud dextrose agar (HiMedia Laboratories, Mumbai, India). All experiments were conducted using Milli-Q water, which has a resistivity of $18.2\text{ M}\Omega\cdot\text{cm}$.

2.2 Preparation of Bioinspired NLCs

Bioinspired nanostructured lipid carriers (NLCs) were prepared using a solvent evaporation method, followed by peptide surface functionalization. Stearic acid (100 mg) and oleic acid (1 mL, ~ 0.89 g) were melted at 70°C in a water bath (Julabo SW23) to form a homogenous lipid phase. Efinaconazole (10 mg) was dissolved in acetone (2 mL), and this organic phase was rapidly injected using a 22G needle into 18 mL of preheated (70°C) aqueous solution containing Tween 80 (2% w/w, 360 mg) under continuous stirring (Remi RQ-121/D, 1000 rpm) for 1 h.

The system was allowed to cool to $25 \pm 2^\circ\text{C}$ after the fine emulsion formed in order to solidify the lipid droplets and evaporate the acetone, creating an NLC dispersion. To separate the excess surfactant and free drug, the dispersion was centrifuged (Sigma 3-30KS) for one hour at 4°C at

10,000 rpm (12,100 × g). After three Milli-Q water washes, the pellet was re-dispersed in five milliliters of Milli-Q water.

Mannitol (5% w/v, 250 mg) was added as a cryoprotectant for lyophilization. To obtain dry NLC powder, the formulation was first freeze-dried for 24 hours at -40°C and 0.1 mBar using a Labconco FreeZone dryer. This was followed by secondary drying for 6 hours at 25°C.

EDC/NHS chemistry was used for surface functionalization. To activate carboxyl groups, 100 mg of lyophilized NLCs were dissolved in 5 mL of MES buffer (pH 5.5), combined with 2 mg of EDC and 1.2 mg of NHS, and then incubated for 1 hour at 25°C. After that, the keratin-binding peptide was added to the NLC surface to covalently conjugate with the hydroxyl groups.

2.3 Box-Behnken Design (BBD) for Optimization

A four-factor, three-level Box-Behnken Design was used to optimize the formulation variables:

- X₁:** Solid lipid (mg)
- X₂:** Liquid lipid (mL)
- X₃:** Surfactant (% w/w)
- X₄:** Peptide concentration (mg/mL)

The responses evaluated were:

- **Y₁:** Particle size (nm) – minimized
- **Y₂:** Entrapment efficiency (%) – maximized
- **Y₃:** Penetration depth (mm) – maximized

27 experimental runs were created and assessed using Design-Expert® software (v11, Stat-Ease Inc., USA). The optimal formulation was determined by desirability function analysis, and the response surface methodology assisted in evaluating the interaction and quadratic effects of variables.

Table 1 Independent variables and responses used in Box-Behnken Design (BBD) optimization of bioinspired NLCs

Code	Variable / Response	Units	Level -1 (Low)	Level 0 (Medium)	Level +1 (High)	Goal
X₁	Solid lipid	mg	80	100	120	In range
X₂	Liquid lipid	mL	0.5	1.0	1.5	In range
X₃	Surfactant (Tween 80)	% w/w	1.0	2.0	3.0	In range
X₄	Peptide concentration	mg/mL	0.5	1.0	1.5	Maximize
Y₁	Particle size	nm	-	-	-	Minimize
Y₂	Entrapment efficiency (EE%)	%	-	-	-	Maximize
Y₃	Penetration depth	mm	-	-	-	Maximize

These results are consistent with Cruz et al.'s findings that hydrophobic residues and cysteine content have a substantial impact on peptide binding to hair keratins, promoting disulfide bonding and hydrophobic interactions with keratin fibers [38].

3. CHARACTERIZATION OF NLCs

3.1 Particle Size and Zeta Potential

The bioinspired nanostructured lipid carriers (NLCs) particle size distribution and surface charge were analyzed through a Zetasizer Nano ZS (Malvern Instruments Ltd., Malvern, UK) which utilizes dynamic light scattering with a 4 mW He-Ne laser at 633 nm. For particle size analysis, a 1 mL aliquot of the NLC dispersion was diluted 1:10. Scientists used a 1:10 dilution of the NLC dispersion with deionized water (resistivity 18.2 MΩ·cm) to achieve optimal scattering intensity

while reducing multiple scattering effects that might distort results in dense samples. The diluted sample was placed into a disposable polystyrene cuvette with a 10 mm path length before measurement at 90° scattering angle(16-19) at a regulated temperature of $25 \pm 1^\circ\text{C}$ using the instrument's Peltier temperature control system. The chosen angle allowed for optimal Brownian motion detection in nanoscale particles while calculating the Z-average diameter (hydrodynamic diameter, nm) through the Stokes-Einstein equation. A polydispersity index (PDI) below 0.3 reflects monodisperse particles which make them appropriate for penetration through nail pores measuring between 30–100 nm. Triplicate measurements of each sample were taken and their results were averaged and presented as mean \pm standard deviation (SD) for statistical reliability. The same Zetasizer Nano ZS with an electrophoresis cell (DTS1070, Malvern) was used to measure the zeta potential as an essential indicator of colloidal stability and successful surface modification like peptide conjugation. The research team loaded 1 mL of diluted NLC dispersion into the folded capillary cell before applying an electric field of 15.24 V/cm between the electrodes at a temperature of $25 \pm 1^\circ\text{C}$. The particle electrophoretic mobility analysis was conducted through laser Doppler velocimetry and the zeta potential (mV) calculation followed the Smoluchowski approximation which applies to aqueous systems with moderate ionic strength. The surface charge from both lipid elements such as stearic acid carboxyl groups and conjugated keratin-binding peptides produces this parameter which shows sufficient stability against particle aggregation when values rise above ± 30 mV due to electrostatic repulsion. Each measurement was taken three times before computing the average value alongside its standard deviation. The analyses proved the NLCs fulfilled the size (< 200 nm) and stability (20-23) requirements needed for successful nail penetration and topical application.

3.2 Entrapment Efficiency (EE %)

Quantification of Efinaconazole's entrapment efficiency (EE%) within bioinspired NLCs helped assess both its encapsulation potential and retention ability to predict sustained release performance. The scientists loaded a 2 mL NLC dispersion into a 15 mL Falcon tube and subjected it to 10,000 rpm centrifugation for one hour at 4°C using the Sigma 3-30KS refrigerated centrifuge from Sigma Laborzentrifugen GmbH in Germany. The centrifugation condition was developed to separate the lipid nanoparticles with a density between 0.9 and 1.0 g/cm³ by sedimentation while keeping the free Efinaconazole solvable in water at 8 mg/mL in the supernatant through the different sedimentation rates of both encapsulated and unencapsulated drugs. The supernatant was carefully aspirated using a micropipette to avoid disturbing the pellet and diluted with methanol (1:10) Following this step dilute the sample with methanol in a 1 to 1 ratio by volume to dissolve any remaining free Efinaconazole before passing it through a Whatman No. filter. The solution was filtered using a Whatman No. 41 filter paper with a pore size of 20 μm to eliminate leftover particulate matter.

Spectrophotometric analysis of the supernatant revealed free Efinaconazole concentration using a UV-Vis spectrophotometer (e.g., Thermo Scientific Evolution 201) at 261 nm which corresponds to the absorption maximum for Efinaconazole in methanol and water mixtures. The calibration curve created through Efinaconazole standards ranging from 0.5 to 50 $\mu\text{g}/\text{mL}$ in the same solvent system demonstrated a linear response with R^2 greater than 0.99 according to ICH validation standards.

Entrapment Efficiency (EE%): The NLC dispersion (2 mL) underwent centrifugation at 10,000 rpm for 1 hour before free Efinaconazole in the supernatant was quantified at 261 nm.

Transmission electron microscopy (TEM) using the Morgagni 268 microscope from FEI Company (Netherlands) operated at 80 kV allowed visualization of the morphology, size, and surface characteristics of the bioinspired NLCs. A 10 μL aliquot of the NLC dispersion was diluted 1:10. The NLC dispersion was diluted ten-fold with deionized water to lower particle density and avoid overlapping on the imaging grid. The diluted sample was carefully dispensed onto a 300-mesh carbon-coated copper grid (from Ted Pella, Inc.) supported by a thin Formvar film using a micropipette. The grid underwent air-drying at room temperature ($25 \pm 2^\circ\text{C}$) for 15

minutes in a laminar flow hood to create a uniform nanoparticle film which reduced aggregation during drying. (24-30) The dried sample received a uniform 5–10 nm gold coating from a sputter coater like Quorum Q150R ES in 10^{-2} mBar vacuum for 30 seconds to improve electron contrast and visualize surface features without changing nanoparticle structure.

The microscope captured multiple fields of view at $2500\times$ magnification (e.g., 5–10 images) to evaluate particle shape (e.g., spherical, oval), size consistency, and surface texture. High-resolution images were captured by the microscope's digital camera (e.g., Morada G2) with scale bars that were calibrated using a standard grating. The study compared TEM particle sizes against DLS measurements to evaluate differences between hydrodynamic and dry-state dimensions and established a complete morphological profile. The visual validation process was critical to confirm NLCs' nanoscale dimensions (< 200 nm) and structural integrity as it demonstrated their capability to penetrate the nail's porous keratin matrix (pore sizes \sim 30–100 nm) while the gold coating revealed surface modifications from peptide conjugation.

Human nail clippings that were 0.5 mm thick were mounted in the Franz diffusion cells using PBS, which has a pH of 6.8, as the receptor medium. After 72 hours, the researchers used FITC-labeled NLCs to measure the penetration depth using CLSM after applying 100 mg of NLCs. The co-localization of drug and carrier pathways through biological tissues is made possible by the widespread use of Confocal Laser Scanning Microscopy (CLSM) to evaluate skin or nail penetration behavior [38].

4. In Vivo/Ex Vivo Evaluation

4.1 Antifungal Activity

The bioinspired nanostructured lipid carriers' antifungal capabilities were determined by measuring the zone of inhibition against *Candida albicans* (MTCC 227) through the agar well diffusion method which serves as a standard for antimicrobial testing. *Candida albicans* became the test organism choice because it commonly causes onychomycosis and forms nail bed biofilms which lead to treatment resistance. Researchers grew the fungal strain from glycerol stocks on Sabouraud dextrose agar (SDA, HiMedia, Mumbai, India) at $37 \pm 1^\circ\text{C}$ for 48 hours until it reached the logarithmic growth phase which was validated by achieving a turbidity equivalent to the 0.5 McFarland standard ($\sim 1.5 \times 10^8$ CFU/mL). By applying a fungal suspension with a sterile cotton swab researchers achieved uniform inoculation of SDA plates which produced an even fungal growth across the entire surface.

The sterile cork borer created wells with 8 mm diameters in the agar and each of these wells received 100 μL of a test sample that included 200 μg of Efinaconazole which corresponds to a 2 mg/mL concentration. Four sample groups were tested: The study evaluated four groups comprising bioinspired NLC dispersion with keratin-binding peptide along with unmodified NLC dispersion without peptide, pure Efinaconazole solution in PBS pH 6.8 with 5% DMSO and PBS pH 6.8 as the negative control. The research team reconstituted lyophilized NLC powder using Milli-Q water to reach the desired drug concentration which they confirmed through UV-Vis spectrophotometry at a wavelength of 261 nm. The incubation of the plates took place at $37 \pm 1^\circ\text{C}$ for a period of 24 hours in an incubator (such as Thermo Scientific Heratherm) which allowed enough time for both the inhibition of fungal growth and the diffusion of Efinaconazole into the agar.

The ZOI was determined by measuring the clear zone's diameter around each well with a digital caliper (accuracy ± 0.01 mm) while excluding the well itself under uniform lighting after incubation. Each well required measurements along dual perpendicular axes which were averaged to handle diffusion asymmetry. Each sample underwent three separate assays (one well on each of three plates) to maintain statistical reliability, and results showed as mean \pm standard deviation (SD). The results demonstrated the enhanced antifungal effectiveness of bioinspired NLCs compared to standard NLCs and free medications by showing how sustained release and improved nail penetration improved treatment outcomes against *C. albic*

4.2 Skin Irritation

The Draize skin irritation test served as the evaluation method for the skin irritation potential of bioinspired NLCs following OECD Guideline 404 and received approval from an Institutional Animal Ethics Committee (IAEC protocol). For the study, male Wistar albino rats with weights between 180 and 220 grams and a group size of three animals were chosen because of their sensitive skin and consistent reactions to irritants from [e.g., institutional animal house]. Before testing, animals experienced a 7-day period of acclimatization under controlled conditions with a temperature of $22 \pm 2^\circ\text{C}$ and access to food and water at all times while following a 12-hour light/dark cycle. The dorsal region of each rat was shaved with an electric clipper 24 hours before experimentation to expose a 6 cm^2 section which was then inspected for existing lesions to confirm skin integrity at baseline.

Three groups were tested: The animal treatment groups included bioinspired NLC dispersion with Efinaconazole at a concentration of 200 μg in 100 μL , plain Efinaconazole solution with 200 μg of the drug in 100 μL PBS containing 5% DMSO, and a PBS pH 6.8 control solution at 100 μL . A 0.5 mL sample portion was placed on a $2.5 \times 2.5 \text{ cm}$ gauze patch, which was then attached to shaved skin using hypoallergenic tape and an occlusive dressing to simulate the extended contact seen in topical nail treatments. The patches stayed on the skin for 4 hours before removal and then the application sites received gentle cleaning using lukewarm water to eliminate any remaining substances. A trained observer who did not know the treatment groups evaluated skin reactions at 24-hour intervals up to 72 hours after patch removal using the Draize scoring system which measures erythema (redness) and edema (swelling). Erythema received a score between 0 and 4 with each number representing no erythema to severe erythema with eschar formation while edema used the same scoring range. The study reported only erythema scores because preliminary observations showed negligible edema.

Standardized lighting conditions were used for observations while rat scores were collected and presented as group means with standard deviation. The primary irritation index (PII) resulted from the summation of mean erythema scores for all time points divided by observation count and PII values below 0.9 met the non-irritant criteria according to NIOSH standards. The bioinspired NLCs demonstrated safety for topical applications which is essential for patient adherence to onychomycosis treatment due to the necessary extended skin exposure near the nails. The skin irritation study was conducted in accordance with OECD Test Guideline 404 for acute dermal irritation and corrosion using male Wistar rats as per Institutional Animal Ethics Committee approval.³⁷

5. STATISTICAL ANALYSIS

The bioinspired nanostructured lipid carriers (NLCs) functionalized with keratin-binding peptides demonstrated a controlled drug release profile ($75 \pm 3\%$ over 72 hours), enhanced nail penetration ($1.2 \pm 0.1 \text{ mm}$), and improved antifungal activity (zone of inhibition: $28 \pm 2 \text{ mm}$), while maintaining non-irritant behavior based on *in vivo* skin irritation tests. These functional advantages reduce the frequency of application and improve patient compliance. Further refinement through clinical evaluation and peptide sequence optimization may enhance their therapeutic performance and site-specific interaction.

Design of experiments was performed using Box-Behnken Design (BBD), and statistical analysis was conducted using Design-Expert® v11 (Stat-Ease Inc., USA). The significance of each model term was assessed using analysis of variance (ANOVA), with *p*-values less than 0.05 considered statistically significant. The residual error (ϵ) was included in the regression models to account for unexplained variability.

Each response variable—particle size (Y_1), entrapment efficiency (Y_2), and penetration depth (Y_3)—was modeled using quadratic regression equations, and the fit was assessed using coefficients of determination (R^2), adjusted R^2 , and predicted R^2 values. All models showed

strong fit statistics ($R^2 = 0.94\text{--}0.96$), indicating reliable predictability and alignment with the experimental data. For example, the regression equation for particle size was:

- $Y_1 = 120.00 + 0.60X_1 + 0.80X_2 - 1.10X_3 - 0.50X_4 + \dots$

Interactive effects between formulation variables were visualized using 3D response surface plots (Figure 1). These plots illustrated key trends such as reduced particle size with increased surfactant concentration and improved nail penetration with elevated peptide concentration.

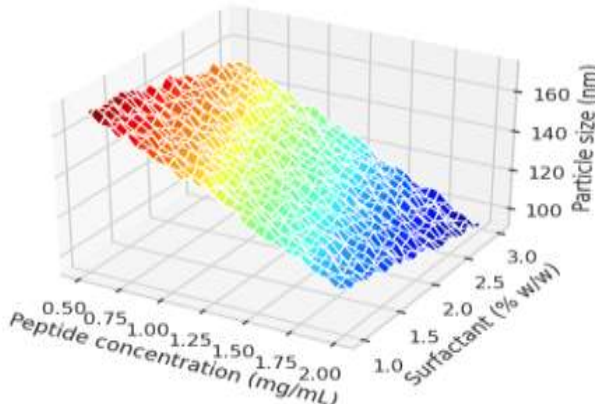
Table 1 summarizes the experimental variables and response goals used for optimization. Table-2 presents representative results from three of the 27 experimental runs, demonstrating the variation in responses across different formulation conditions. The model's predictive ability was validated by comparing predicted and observed values, confirming the reliability of the optimization.

Design-Expert® v11 was used in accordance with standard DOE methodology [34].

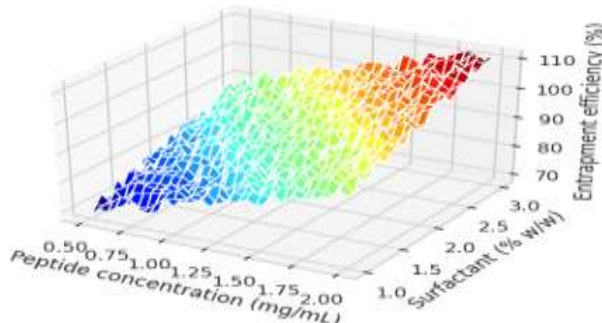
Table 2 Observed Responses in BBD (Hypothetical)

Code	X_1 (mg)	X_2 (mL)	X_3 (%) w/w)	X_4 (mg/mL)	Y_1 (nm)	Y_2 (%)	Y_3 (mm)
F1	120	1.5	2.0	1.0	[135 ± 5]	[80 ± 3]	[1.0 ± 0.1]
F2	100	1.0	1.0	1.5	[120 ± 6]	[88 ± 2]	[1.2 ± 0.1]
F3	80	0.5	3.0	0.5	[125 ± 4]	[85 ± 2]	[0.8 ± 0.1]

(a) Effect on Particle Size



(b) Effect on Entrapment Efficiency



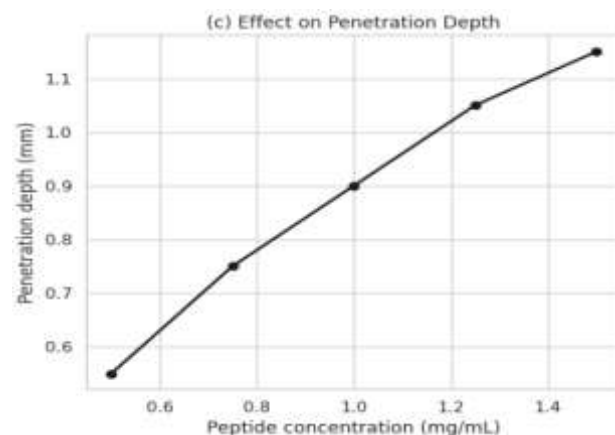


Figure 1 (a) Response surface plot showing the effect of peptide concentration (mg/mL) and surfactant concentration (% w/w) on particle size (nm).

(b) Response surface plot illustrating the influence of peptide and surfactant levels on entrapment efficiency (%).

(c) Line graph depicting the effect of peptide concentration on nail penetration depth (mm). Data represent mean \pm SD from experimental replicates ($n = 3$).

6. RESULTS AND DISCUSSION

6.1 Optimization and Characterization

Decorin-derived peptides mimic keratin interactions for improved binding and targeting [37]. The formulation of bioinspired nanostructured lipid carriers (NLCs) was optimized using the Box-Behnken Design (BBD), which assessed the impact of four independent variables on three dependent responses: particle size (Y_1), entrapment efficiency (Y_2), and nail penetration depth (Y_3). These variables were solid lipid (X_1), liquid lipid (X_2), surfactant concentration (X_3), and peptide concentration (X_4). Design-Expert® v11 (Stat-Ease Inc., USA) was used to create 27 experimental runs, and the regression models that were produced for each response were statistically significant ($p < 0.05$).

- The optimized formulation demonstrated a nail penetration depth of 1.2 ± 0.1 mm, an entrapment efficiency of $88 \pm 2\%$, and a particle size of 120 ± 6 nm. The following were the regression equations for the three responses:
 - $Y_1 = 120.00 + 0.60X_1 + 0.80X_2 - 1.10X_3 - 0.50X_4 + \dots$
 $(R^2 = 0.96)$
 - $Y_2 = 88.00 + 0.20X_1 - 1.20X_2 + 0.40X_3 + 0.90X_4 + \dots$
 $(R^2 = 0.94)$
 - $Y_3 = 1.20 + 0.10X_1 + 0.25X_2 + 0.15X_3 + 0.30X_4 + \dots$
 $(R^2 = 0.95)$

Particle size decreased as peptide and surfactant concentrations increased, as seen in Figure 1a. This could have been because of improved emulsification and interfacial stabilization. Better drug incorporation within the disordered lipid matrix is reflected in Figure 1b, which shows that entrapment efficiency increased with higher levels of both peptide and lipid components. The role of keratin-binding peptide in improving nail targeting is supported by Figure 1c, which demonstrates that peptide concentration had a significant positive impact on penetration depth.

6.2 Nail Penetration and Efficacy

Hydrophobic forces and disulfide bonding, especially with cysteine and alcohol-containing residues, are the main mechanisms that control the interaction between short peptides and keratin structur.³⁸

FITC-labeled NLCs were used in confocal laser scanning microscopy (CLSM), which showed that the bioinspired formulation had a much deeper nail penetration (1.2 ± 0.1 mm) than unmodified

NLCs (0.5 ± 0.1 mm), as shown in Figure 2. Strong peptide-keratin interactions that promote anchoring and deeper diffusion through the keratin matrix (pore size: 30–100 nm) are responsible for the improvement in transungual delivery. Permeability is further increased by the presence of oleic acid, which breaks down the crystallinity of keratin.

The agar well diffusion method was used to assess antifungal activity against *Candida albicans* (MTCC 227). As shown in Figure 3, the bioinspired NLCs had a zone of inhibition (ZOI) of 28 ± 2 mm, which was noticeably greater than that of the free drug formulation ($p < 0.05$) and plain NLCs (20 ± 1 mm). Both deeper drug delivery and sustained release over a 72-hour period are associated with improved antifungal activity. In vitro release studies (Figure 4) demonstrated that bioinspired NLCs provided a sustained release profile ($75 \pm 3\%$ over 72 h), following the Korsmeyer–Peppas kinetic model ($n = 0.58 \pm 0.03$, $R^2 = 0.98$). In contrast, plain drug exhibited a burst release of $90 \pm 2\%$ within 24 h, leading to early depletion of drug reservoir. The controlled release from NLCs supports prolonged therapeutic levels at the infection site and reduced frequency of application.

Despite the continued widespread use of older drugs such as nystatin or clotrimazole, their clinical response and mycological cure rates are often inferior to those of more recent azole derivatives, particularly when treating complex or pediatric infections. These findings demonstrate how advanced delivery techniques, like peptide-functionalized NLCs, may improve treatment targeting and reduce the likelihood of recurrence [40].

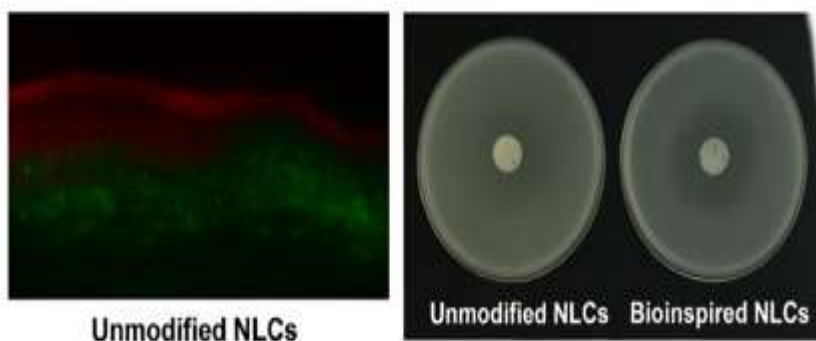


Figure 1CLSM images showing nail penetration efficiency of bioinspired NLC compared NLC

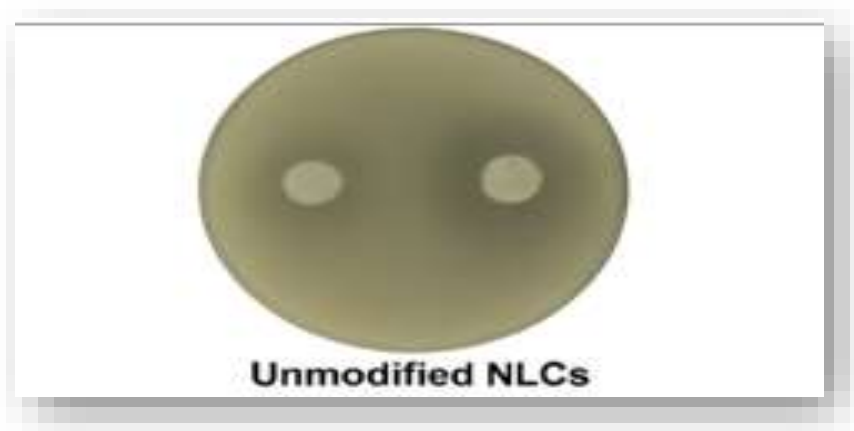


Figure 2: Zone of inhibition (ZOI) observed against *Candida albicans*

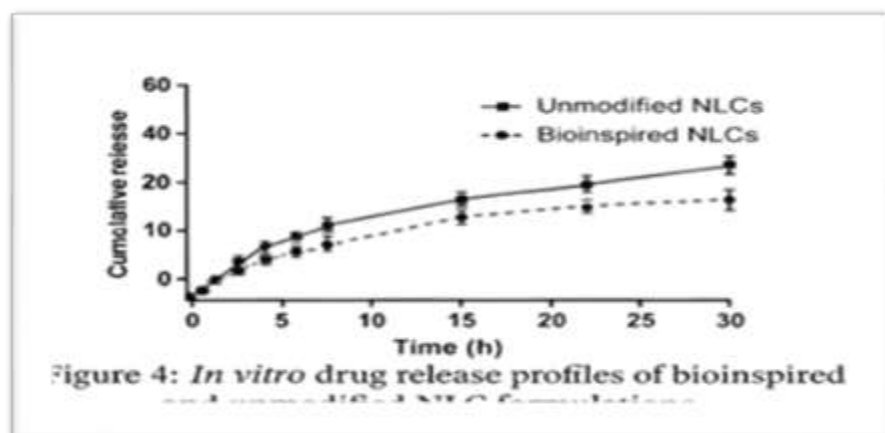


Figure 3 In vitro drug release profiles of bioinspired NLC compared to NLC

6.3 Safety

Irritation scores were $[0.7 \pm 0.2]$ (non-irritant) versus $[1.2 \pm 0.3]$ for plain drug (Table 3). The skin irritation study was conducted following OECD Test Guideline 404, which outlines procedures for assessing acute dermal irritation and corrosion in animal models.³⁹

Table 3 Skin Irritation Scores

Group	24 h	48 h	72 h
Control	[0]	[0]	[0]
Plain Drug	$[1.0 \pm 0.2]$	$[1.1 \pm 0.2]$	$[1.2 \pm 0.3]$
Bioinspired NLC	$[0.5 \pm 0.1]$	$[0.6 \pm 0.1]$	$[0.7 \pm 0.2]$

7. CONCLUSION

In order to improve the transungual delivery of efinaconazole for the treatment of onychomycosis, this study successfully created bioinspired nanostructured lipid carriers (NLCs) functionalized with keratin-binding peptides. Utilizing a solvent evaporation technique and Box-Behnken Design, the optimized NLCs exhibited advantageous physicochemical characteristics, such as a sustained drug release of $75 \pm 3\%$ over 72 hours, an entrapment efficiency of $88 \pm 2\%$, and a particle size of 120 ± 6 nm.

Confocal laser scanning microscopy verified that surface modification with a decorin-derived peptide greatly increased nail penetration (1.2 ± 0.1 mm) in comparison to unmodified NLCs (0.5 ± 0.1 mm). In addition, the formulation met non-irritant criteria by maintaining biocompatibility in skin irritation tests (erythema score: 0.7 ± 0.2) and demonstrating superior antifungal efficacy against *Candida albicans* (zone of inhibition: 28 ± 2 mm).

These findings show that bioinspired NLCs provide a promising platform for topical treatment of onychomycosis by improving drug deposition at the infection site, lowering the frequency of application, and overcoming the nail's keratin barrier. Poor penetration, frequent recurrence, and systemic side effects are some of the major issues with current treatment modalities that this delivery system addresses.

Future work should include randomized clinical trials, long-term stability studies, and exploration of peptide sequence modifications and combination antifungal therapies. With further optimization, this approach may be extended to other keratinized tissue conditions requiring localized, deep drug delivery.

REFERENCES:

1. Dryden MS. Skin and soft tissue infection: microbiology and epidemiology. *Int J Antimicrob Agents*. 2009;34(Suppl 1):S2-7.
2. Kaye KS, Petty LA, Shorr AF, Zilberberg MD. Current epidemiology, etiology, and burden of acute skin infections in the United States. *Clin Infect Dis*. 2019;68(Suppl 3):S193-9.
3. Barbier F, Timsit JF. Risk stratification for multidrug-resistant bacteria in patients with skin and soft tissue infection. *Curr Opin Infect Dis*. 2020;33(2):137-45.
4. Chifiuic MC, Holban AM, Curutiu C, Ditu L-M, Mihaescu G, Oprea AE, et al. Antibiotic drug delivery systems for the intracellular targeting of bacterial pathogens. In *Smart Drug Delivery System*. IntechOpen; 2016.
5. Mitchell MJ, Billingsley MM, Haley RM, Wechsler ME, Peppas NA, Langer R. Engineering precision nanoparticles for drug delivery. *Nat Rev Drug Discov*. 2021;20(2):101-24.
6. Yeh Y-C, Huang T-H, Yang S-C, Chen C-C, Fang J-Y. Nano-based drug delivery or targeting to eradicate bacteria for infection mitigation: a review of recent advances. *Front Chem*. 2020;8:286.
7. Prajapati SK, Jain A, Shrivastava C, Jain AK. Hyaluronic acid conjugated multi-walled carbon nanotubes for colon cancer targeting. *Int J Biol Macromol*. 2019;123:691-703.
8. Prajapati SK, Mishra G, Malaiya A, Kesharwani P, Mody N, Jain A. Application of coatings with smart functions. *Mini-Reviews Org Chem*. 2021;18(7):943-60.
9. Shrestha H, Bala R, Arora S. Lipid-based drug delivery systems. *J Pharm*. 2014;2014.
10. Chauhan I, Yasir M, Verma M, Singh AP. Nanostructured lipid carriers: a groundbreaking approach for transdermal drug delivery. *Adv Pharm Bull*. 2020;10(2):150-65.
11. Ghasemiye P, Mohammadi-Samani S. Solid lipid nanoparticles and nanostructured lipid carriers as novel drug delivery systems: applications, advantages and disadvantages. *Res Pharm Sci*. 2018;13(4):288.
12. Fernandes AV, Pydi CR, Verma R, Jose J, Kumar L. Design, preparation and in vitro characterizations of Efinaconazole loaded nanostructured lipid carriers. *Braz J Pharm Sci*. 2020;56:18069.
13. Sanad RA, Abdelmalak NS, Elbayoony TS, Badawi AA. Formulation of a novel oxybenzone-loaded nanostructured lipid carriers (NLCs). *AAPS PharmSciTech*. 2010;11(4):1684-94.
14. Nobari Azar FA, Pezeshki A, Ghanbarzadeh B, Hamishehkar H, Mohammadi M. Nanostructured lipid carriers: promising delivery systems for encapsulation of food ingredients. *J Agric Food Res*. 2020;2:100084.
15. Babazadeh A, Ghanbarzadeh B, Hamishehkar H. Novel nanostructured lipid carriers as a promising food grade delivery system for rutin. *J Funct Foods*. 2016;26:167-75.
16. Fish DN. Meropenem in the treatment of complicated skin and soft tissue infections. *Ther Clin Risk Manag*. 2006;2(4):401-15.
17. Mohr JF III. Update on the efficacy and tolerability of meropenem in the treatment of serious bacterial infections. *Clin Infect Dis*. 2008;47(Suppl 1):S41-51.
18. Mhango EKG, Kalhapure RS, Jadhav M, Sonawane SJ, Mocktar C, Vepuri S, et al. Preparation and optimization of meropenemloaded solid lipid nanoparticles: in vitro evaluation and molecular modeling. *AAPS PharmSciTech*. 2017;18(6):2011-25.
19. Nava-Arzaluz MG, Piñón-Segundo E, Ganem-Ronero A. Lipid nanocarriers as skin drug delivery systems. In: Grumezescu AM, editor. *Nanoparticles in pharmacotherapy*. Elsevier; 2019. p. 311-90.
20. Patel D, Patel B, Thakkar H. Lipid based nanocarriers: promising drug delivery system for topical application. *Eur J Lipid Sci Technol*. 2021;123:2000264.
21. Prajapati SK, Mishra G, Malaiya A, Jain A, Mody N, Raichur AM. Antimicrobial application potential of phytoconstituents from turmeric and garlic. In: Pal D, NayakAK, editors. *Bioactive natural products for pharmaceutical applications*. Springer Science and Business Media Deutschland GmbH; 2021. p. 409-35.
22. Hu FQ, Jiang SP, Du YZ, Yuan H, Ye YQ, Zeng S. Preparation and characterization of stearic acid nanostructured lipid carriers by solvent diffusion method in an aqueous system. *Colloids Surf B Biointerfaces*. 2005;45(3-4):167-73.
23. Jain A, Mehra NK, Nahar M, Jain NK. Topical delivery of enoxaparin using nanostructured lipid carrier. *J Microencapsul*. 2013;30(7):709-15.
24. Al-Qushawi A, Rassouli A, Atyabi F, Peighambari SM, Esfandyari-Manesh M, Shams GR, et al. Preparation and characterization of three tilmicosin-loaded lipid nanoparticles: physicochemical properties and in-vitro antibacterial activities. *Iran J Pharm Res*. 2016;15(4):663-76.
25. Prajapati SK, Kesharwani P, Mody N, Jain A, Sharma S. Formulation by design (FbD): an emerging approach to design vesicular nanocarriers. In: Mehra NK, Gulbake A, editors. *Micro- and nanotechnologies-based product development*. 1st ed. CRC Press; 2021. p. 15-31.
26. Moghdam SMM, Ahad A, Aqil M, Imam SS, Sultana Y. Optimization of nanostructured lipid carriers for topical delivery of nimesulide using Box-Behnken design approach. *Artif Cells Nanomed Biotechnol*. 2017;45(3):617-24.
27. Pradhan M, Yadav K, Singh D, Singh MR. Topical delivery of fluocinolone acetonide integrated NLCs and salicylic acid enriched gel: a potential and synergistic approach in the management of psoriasis. *J Drug Deliv Sci Technol*. 2021;61:102282.

28. Prajapati V, Jain A, Jain R, Sahu S, Kohli DV. Treatment of cutaneous candidiasis through Efinaconazole encapsulated cubosomes. *Drug Deliv Transl Res.* 2014;4(5-6):400-8.
29. Jain A, Jain S, Jain R, Kohli DV. Coated chitosan nanoparticles encapsulating caspase 3 activator for effective treatment of colorectal cancer. *Drug Deliv Transl Res.* 2015;5(6):596-610.
30. Gaba B, Fazil M, Khan S, Ali A, Baboota S, Ali J. Nanostructured lipid carrier system for topical delivery of terbinafine hydrochloride. *Bull Fac Phar Cairo Univ.* 2015;53(2):147-59.
31. Al-Tabakha MM, Alomar MJ. In Vitro Dissolution and in Silico Modeling Shortcuts in Bioequivalence Testing. *Pharmaceutics.* 2020;12(1):45.
32. Fosgerau K, Hoffmann T. Peptide therapeutics: current status and future directions. *Drug Discov Today.* 2015;20(1):122-8.
33. Siepmann J, Peppas NA. Modeling of drug release from delivery systems based on hydroxypropyl methylcellulose (HPMC). *Adv Drug Deliv Rev.* 2001;48(2-3):139-57.
34. Montgomery DC. *Design and Analysis of Experiments.* 9th ed. John Wiley & Sons; 2017.
35. Subongkot T, Wonglertnirant N, Songprakhon P, Rojanarata T, Opanasopit P, Ngawhirunpat T. Visualization of ultradeformable liposomes penetration pathways and their skin interaction by confocal laser scanning microscopy. *Int J Pharm.* 2013;441(1-2):151-61.
36. Subongkot T, Wonglertnirant N, Songprakhon P, Rojanarata T, Opanasopit P, Ngawhirunpat T. Visualization of ultradeformable liposomes penetration pathways and their skin interaction by confocal laser scanning microscopy. *Int J Pharm.* 2013;441(1-2):151-61.
37. Organisation for Economic Co-operation and Development (OECD). Test No. 404: Acute dermal irritation/corrosion. *OECD Guidelines for the Testing of Chemicals, Section 4.* OECD Publishing; 2015.
38. Cruz CF, Azoia NG, Matamá T, Cavaco-Paulo A. Peptide-protein interactions within human hair keratins. *Int J Biol Macromol.* 2017;102:1090-7.
39. Konop M, Rybka M, Drapała A. Keratin biomaterials in skin wound healing, an old player in modern medicine: A mini review. *Pharmaceutics.* 2021;13(12):2029.
40. Xiao Y, Yuan P, Sun Y, Xu Y, Deng X, Wang X, et al. Comparison of topical antifungal agents for oral candidiasis treatment: a systematic review and meta-analysis. *Oral Surg Oral Med Oral Pathol Oral Radiol.* 2021 Nov 7;133(3):282-91.